

Jeremie Peres

I. INTRODUCTION

Human body models (HBMs) will increasingly be used in car safety assessments as a supplemental tool to dummies [1]. However, many challenges remain for a pertinent and standardized application of HBMs in car safety [2-3]. One key aspect is the interaction between the HBM and the safety systems, in particular the seat belt. HBMs tend to be more flexible than dummies, which in combination with very deformable soft tissues leads to an increased level of transverse bending moment applied to the belt webbing. Therefore, it is especially crucial for simulations with HBMs to implement realistic material properties of the seat-belt webbing not only in tension but also in bending. Traditional 2-D membrane element modelling of the belt does not include any bending stiffness. Recently, code-specific features have been implemented to remedy this limitation [4]. Another approach is to add to the membrane elements a layer of shell elements, a solution that would be applicable to any FE-code. However, a clear and validated set of the material properties is not available in the scientific literature. The goal of this paper is to provide such a set of material properties and to observe the effect of the added shell layer in a validated sled environment using a state-of-the-art HBM.

II. METHODS

In a first step, the bending stiffness of a standard belt webbing is determined using a simple experimental test. Secondly, based on the results, the material properties of the shell and membrane layers are identified and validated. Finally, two sled simulations are launched with the THUMS v4.1 model. In the first one, the belt webbing is modelled using a single-membrane elements layer, whereas in the second one it is modelled using a membrane and a shell layer.

Experimental Testing

The Peirce test [5] is typically used to determine the bending stiffness of flexible materials, such as fabrics. It is a cantilever type test that determines the tissue length (l) needed for the sample to bend under its own weight, so that the angle between the horizontal and a line connecting the origin of the cantilever to the tip deflection point reaches a predefined value (in this study 45°). The equivalent bending strength (EI) is calculated analytically using some variation of the beam theory:

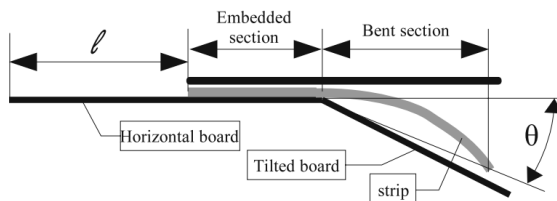


Fig. 1. Illustration of the Peirce test [6].

$$J = EI = wl^3 * \left[\frac{\cos\left(\frac{\theta}{2}\right)}{8 * \tan(\theta)} \right]$$

where w is the mass per unit length of the tested tissue sample, l the length of tissue under bending, and θ the angle described previously.

Eq. 1. Calculation of the bending stiffness according to Peirce.

Computational Modelling

The membrane layer is modelled using LS-DYNA material type B01_SEATBELT, with a curve defining the tensile properties. An elastic material model is used for the shell layer. From the previously determined bending stiffness and for a given webbing thickness and width, the Young's modulus of the shell elements can be determined. When using two element layers, the stiffness in tension of the membrane elements must be reduced to counterbalance the added stiffness of the shell layer. This is done by reproducing a tensile test and adjusting the material properties (curve scaling factor). Once the material properties of both layers are calibrated, the Peirce test is reproduced via simulation for validation purposes. A belt sample of length l , fixed in rotation and translation at one end, is positioned horizontally and loaded under its own gravity until it reaches an equilibrium.

PDB is using a rigid frontal sled that includes a deployed airbag, a 3-point belt and a retractor with pretension and a 4 kN load limiter. A corresponding simulation model has been validated with several dummy models. Simulation results with the THUMS v4.1 in this environment and with the two belt webbing variants will be compared (belt force, dummy-like outputs, and strain distribution in the ribcage).

III. INITIAL FINDINGS

A bending stiffness of $0.081 \text{ kN}\cdot\text{mm}^2$ was calculated based on the results of the Peirce test ($l=100 \text{ mm}$). The

calibrated material properties of the belt webbing are presented in Table I, the stiffness of the membrane elements was scaled down to achieve the same tensile behaviour as the variant with only membrane elements.

TABLE I
CALIBRATED PARAMETERS OF THE MEMBRANE AND SHELL LAYERS

Membrane thickness (mm)	Membrane stiffness SF (mm)	Shell thickness (mm)	Shell Young's Modulus (GPa)
1.2	0.95	0.6	0.1

Figure 2 shows the results of the tensile tests with the two belt webbing variants. Figure 3 shows the position of the belt webbing at the end of the Peirce test simulations ($l=100$ mm) with different shell stiffness. The variant with a Young's modulus of 0.1 GPa is the closest to the target surface (45° orientation), therefore validating the material properties of the shell layer.

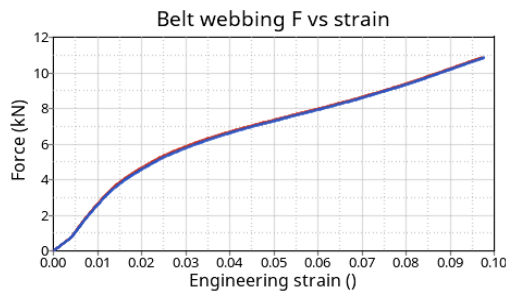


Fig. 2. Tensile test. Blue: Membr. + Shell.
Red: Only membr.

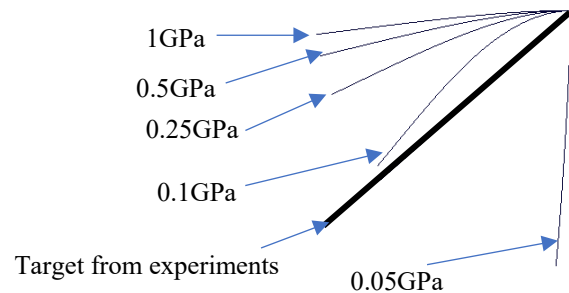


Fig. 3. Simulation of Peirce test with various Young's modulus.

In the sled simulations with the single membrane layer modelling, lap and shoulder belts fold unrealistically due to the lack of bending stiffness. This is not observed for the simulation with the additional shell layer. The differences observed in the belt forces, the dummy-like outputs (Ex: chest acceleration, femur forces...) are negligible between the two belt webbing modelling approaches. However, significant differences are observed when comparing the strain distribution in the ribcage, as illustrated in Fig. 4 and Fig. 5. Due to the unrealistic folding of the belt webbing in the case of the single-membrane layer modelling, the contact surface at the chest is reduced and leads to a more localized loading of the ribs.



Fig. 4. Left 3rd rib 1st max. principal strain distribution for single membrane webbing.

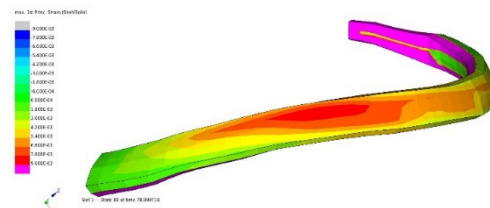


Fig. 5. Left 3rd rib 1st max. principal strain distribution for membrane+shell webbing.

IV. DISCUSSION

The study provides material properties of the belt webbing through experiments and reveals that the transverse bending of belt webbing influences the local contact shape with the HBM chest, and consequently the deformation output. It is particularly important as some efforts are currently being made to implement strain-based injury assessment with HBMs [7-8].

The current study has several limitations. The experimental test was used to determine the longitudinal bending stiffness of the belt band. However, the transverse bending stiffness is more relevant to the type of loading applied to the belt during a sled or a crash simulation. Many parameters, such as friction coefficients, could play a role and potentially affect the conclusions of this study and were not investigated. It is also very likely that the modelling of the flesh and skin in the HBM has a significant effect on the deformation of the belt band, and this should be further investigated, for example by using other HBMs.

V. REFERENCES

- [1] Van Ratingen, M., *IRCOBI*, 2016; [2] Fuchs, T., *et al.*, *IRCOBI*, 2014; [3] Östh, J., *et al.*, *IRCOBI*, 2021; [4] Dahlgren, M., *et al.*, LS-Dyna Users Conference, 2020; [5] Abbott, N. J., *Textil Res J*, 1951; [6] De Bilbao, E., *et al.*, *Exp Mech*, 2010; [7] Forman, J., *et al.*, *AAAM*, 2012; [8] Iraeus, J., *et al.*, *JMBBM*, 2020.